Extreme Mechanics Letters 39 (2020) 100793

Contents lists available at ScienceDirect

Extreme Mechanics Letters

journal homepage: www.elsevier.com/locate/eml

4D printing composite with electrically controlled local deformation

Li-Hua Shao [a,*], Boxuan Zhao [a], Quan Zhang [b], Yufeng Xing [a], Kai Zhang [b,*]

[a] Institute of Solid Mechanics, Beihang University, Beijing 100191, China
[b] School of Aerospace Engineering, Beijing Institute of Technology, Beijing 100081, China

ARTICLE INFO

Article history:
Received 21 January 2020
Received in revised form 22 May 2020
Accepted 23 May 2020
Available online 26 May 2020

Keywords:
4D printing composite
Shape memory polymer
Silver nanowires
Local deformation

ABSTRACT

4D printing holds the important potential for various applications in military, robotics, and healthcare. Among the numerous 4D printed materials, the thermally induced shape memory polymer has been the most used one, which is traditional driven by thermal environments like hot water bath or hot stage. In such way, the whole structure deforms at the same time to transform the shape. However, the environment independent local deformation is required for many applications. In this work, the silver nanowires (Ag-NWs) were employed combining with polylactic acid (PLA) to create a novel electrically driven 4D printing composite. Ag-NWs networks ensured the excellent electric conductivity after repeated tensile and bending deformations. As a result, Ag-NWs could be the excellent "heater" to stimulate the local deformation of PLA under an applied voltage. The theoretical constitutive equations were given, which allowed quantitatively design the structure for desired deformation and property. A biomimetic flower with five petals were demonstrated, that each petal could be controlled independently. An application of the 4D printed structure as a gripper grabbing the cargo in the cold icy environment was realized. Our study has great significance for the future application of shape memory composite materials for multi-functionality in different environments.

1. Introduction

4D printing, which prints smart materials to fabricate three-dimensional objects by a 3D printer [1–3], then the 4D printed structure can change shape or properties versus time under the external stimulus such as heating, vibration and illumination [4,5]. It has been reported that the internal strain stored in the printed material can trigger its shape transformation to create a smart 3D lightweight structures under the external thermal stimulus [5]. This intelligent shape changing could naturally cause the function variation which makes it more attractive in different application prospects, such as aerospace deformation structure [6], temperature indicator [7], biomedical field [8] and smart robot [9,10].

Although the 4D printing materials have made great progresses, there are still some impediments in its further development and application. For the time being, the electroactive polymer [11,12] and shape memory materials [13] are frequently used for 4D printing. Among them, the most deeply studied 4D printing material is the thermally induced shape memory polymer (SMP) [14–16]. The traditional methods to control the deformation of 4D printed SMP structures are water bath heating and hot stage heating. A common disadvantage of these heating methods is the deformation can only occur when the structure is completely surrounded by the thermal environment. What is more, the deformation is overall. However, the local structural deformation is required for many applications, such as mechanical grippers [9,17], self-folding expansion hinges and bionics [18]. In order to solve this problem, various driving methods have been developed, such as electro-thermal [19], illuminated [20] and magnetic driving [10,21]. Among them, the electro-thermal driven method by including the conductive fillers has been the most important one, because it has the advantages of convenient heat generation, easy to drive remotely and adaptable to multi-environments. The metallic particles [22] of Au, Ag and Cu, carbon black [23], carbon nanotubes (CNT) [24], graphene [25] and carbon fiber [26] have been utilized as the conductive fillers in SMP. However, most of the metallic particles are not resistant to the repeated large deformation, and the high expense of the low-producing CNT and graphene is also an impediment for application. Compared to these conductive filling materials, the silver nanowires (Ag-NWs) are easy to aggregate into chains, forming an electroosmotic flow network that is conducive to improve the conductivity of the system [27–29]. Ag-NWs can maintain the excellent electrical conductivity in large deformation and can be mass produced [30,31].

Here, we printed the structure with polylactic acid (PLA) via 3D printer. The Ag-NWs synthesized via chemical liquid polyol

* Corresponding authors.
E-mail addresses: shaolihua@buaa.edu.cn (L.-H. Shao), zhangkai@bit.edu.cn (K. Zhang).

https://doi.org/10.1016/j.eml.2020.100793
2352-4316/

method were uniformly coated into the groove of PLA structure. The obtained PLA/Ag-NWs composite showed fast response under an applied voltage, and took only four seconds from temporary shape to restore the initial shape. Moreover, we studied the deformation mechanism of PLA structure and deduced the corresponding equations, which agreed very well between the theoretical results and the experimental results. For application, a biomimetic flower was fabricated, and the gradual opening of each petal could be realized by controlling the applied voltage. A functional gripper was demonstrated, which could realize the grabbing and releasing the object in cold environment. All of the applications showed the ability of precisely controlled local deformation of the 4D printed PLA/Ag-NWs composite in different environments.

2. Methods

The composite fabrication and functionalization included three steps: (1) Synthesis of Ag-NWs, (2) Combination of Ag-NWs and shape memory polymer, and (3) Electro-thermal experiment, as schematically shown in Fig. 1.

Synthesis of Ag-NWs: Firstly, a mixture of 0.5 g PVP (K30) and 50 ml anhydrous 99.8% ethylene glycol (EG) were heated and thermally stabilized at 180 °C in a magnetically stirred flask with the speed of 350 r/min for 20 mins via Magnetic stirring heating plate (ZNCL-BS, Shanghai, China). Then, added 0.1 ml NaCl in EG solution with the concentration of 0.1 mol/L and heated for 10 mins. Afterwards, dissolved 0.5 g silver nitrate into 50 ml EG and mixed them evenly. Then slowly dripped into the flask through the peristaltic pump tube to avoid spherical or rod-shaped irregular structure, and kept heating for 20 mins. Finally, 100 ml anhydrous 99.8% acetone was added into the cooled solution to get rid of EG, and let it stand for 24 h. Repeated this step for more than three times. After cleaning, the supernatant was poured into the centrifuge tubes, in which 50 ml 99.5% ethanol absolute was added. Then repeated the centrifugation for more than three times to remove the PVP at the speed of 1400 r/min for 17 mins for each time. Finally, the pure Ag-NWs were dispersed in the ethanol solution. The morphological characterization of Ag-NWs was investigated by a Scanning Electron Microscope (SEM, S-4800, Japan), which was shown in the inset of Fig. 1. All of the chemicals used in this work were purchased from Aladdin, China.

Fabrication of the composite structure: The printed material is polylactic acid (PLA) (PolyPlus^{TM} PLA, USA) whose glass transition temperature is about 60 °C. Mechanical properties of PLA including tensile modulus and tensile strength can be found in the literature [32]. All the three-dimensional structures were fabricated by printing PLA materials via MakerBot printer (MakerBot replicator^{+}, Los Angeles, USA). The basic structural unit was a thin beam with the dimension of 60 × 8 × 0.4 mm^3 with a groove of 12 × 8 × 0.1 mm^3 in the middle. The thin beam was placed on a hot plate at 37 °C, and then the Ag-NWs solution was evenly dropped into the groove with a syringe. The solution was magnetically stirred for 2 mins before suction to ensure the Ag-NWs were uniform distributed in the solution. After the Ag-NWs were dry, a very thin layer of the commercial conductive silver paste (CSP, SPI#05001-AB, West Chester, USA) was painted on top of the Ag-NWs for protection. Then the composite structure was left in air for 24 h for complete drying.

Electro-thermal deformation procedure: An appropriate voltage was applied on the thin beam until the glass transition temperature (T_g) of PLA was reached. Afterwards, a temporary shape was constructed by applying an external load till the composite material was cooled down to the room temperature. Turned on the power again, when the temperature reached to T_g under the applied voltage, the structure quickly recovered to its original shape. The temperature of composite structure was measured by an infrared camera (FLIR A655SC, Dresden, Germany) during the experiment. The power supply (SS-3020KD, A-BF, Dongguan, China) was used for applying the voltage. The strain of the beam was measured by the dynamic mechanical analysis (DMA, Electro Force 3200, USA).

3. Results and discussion

Fig. 2(a) illustrates the recovery angle (left) and temperature (right) variations versus the heating time of the thin beam as the inset shown. The obvious slope changes of the curves can be observed. At the beginning, both the decreasing of the recovery angle and the increasing of the temperature are slow, which corresponds to the thermal expansion process. There are dramatically slope changes at the time of 2 s, where the T_g = 60 °C of PLA is reached. Thereafter the temperature increases fast and the deformation rate of the structure is very high, which is corresponding to the phase changing process. Finally, it takes ca. 5 s in total to restore the initial shape of the thin beam. In order to investigate the dependence of the deformation rate on the size of the heater, different dimensions of the Ag-NWs have been coated. As schematically shown in Fig. 2(b), the thickness is constant, and the width is fixed to 8 mm. The angle of the thin beam decreases faster with the larger coated area of Ag-NWs under the applied voltage of 5 V as depicted in Fig. 2(b). The sample was a thin beam with the dimension of 60 × 8 × 0.4 mm^3, and with a groove of 12 × 8 × 0.1 mm^3 in the middle which was coated with Ag-NWs. The temperature changes versus the different applied voltage and the corresponding temperature distributions are illustrated in Figs. 2(c) and 2(d), respectively. Since T_g of PLA is 60 °C, the minimum required voltage is 2.8 V for this sample. In other words, the minimum electric power is ca. 4.704 W to realize the phase change deformation of PLA/Ag-NWs structure.

In order to precisely control the deformation, the detailed deformation equations of SMP were given as follows. For the rectangular thin beam model as shown in Fig. 2, the deformation could be divided into two stages: thermal expansion and shape memory release processes when heated by the applied voltage. The XYZ coordinate system was established along the direction of the beam's length, width and thickness as the inset of Fig. 3(b) shown. According to Tobushi's [33] one-dimensional linear constitutive model based on the classical viscoelastic theory, when $0 < t < t_g$ and $T < T_g$, the thermal expansion strain ε_g of the thermal expansion deformation stage is as follows,

$$\varepsilon_g = \alpha_g \dot{T} t \tag{1}$$

where α_g is the coefficient of thermal expansion, $\dot{T}$ is the heating rate, t is the time and t_g is the time when the temperature reach to T_g.

Because the beam is very thin, which can be simplified as the plane stress problem. The stress is constant along the X axis and varies continuously and uniformly along Z axis. Thus, the thermal expansion bending angle θ is obtained as

$$\theta_1(x, t) = \theta_0 - \frac{2\alpha_g \dot{T} t}{h} x \tag{2}$$

where θ_0 is the initial angle after pre-deformation, h is the thickness of the beam.

As the temperature increasing until $T \geq T_g$, which corresponds to the shape memory stage, the phase change induced strain ε_p is:

$$\varepsilon_p(t_2) = \alpha_{eff} \dot{T} t_2 \tag{3}$$

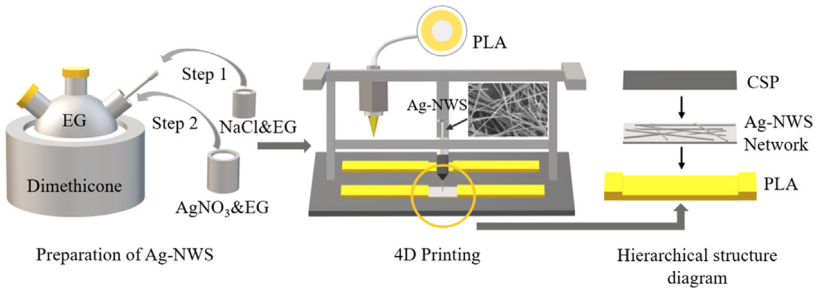

Fig. 1. Schematic plot of the fabrication process of PLA/Ag-NWs composite. Firstly, the Ag-NWs were synthesized via chemical liquid polyol method. The PLA structure was printed by MakerBot^{+} printer and set a groove in the middle of SMP structure, then the Ag-NWs were evenly dropped into the groove. After drying, the Ag-NWs layer was coated with a thin layer of commercial conductive silver paste.

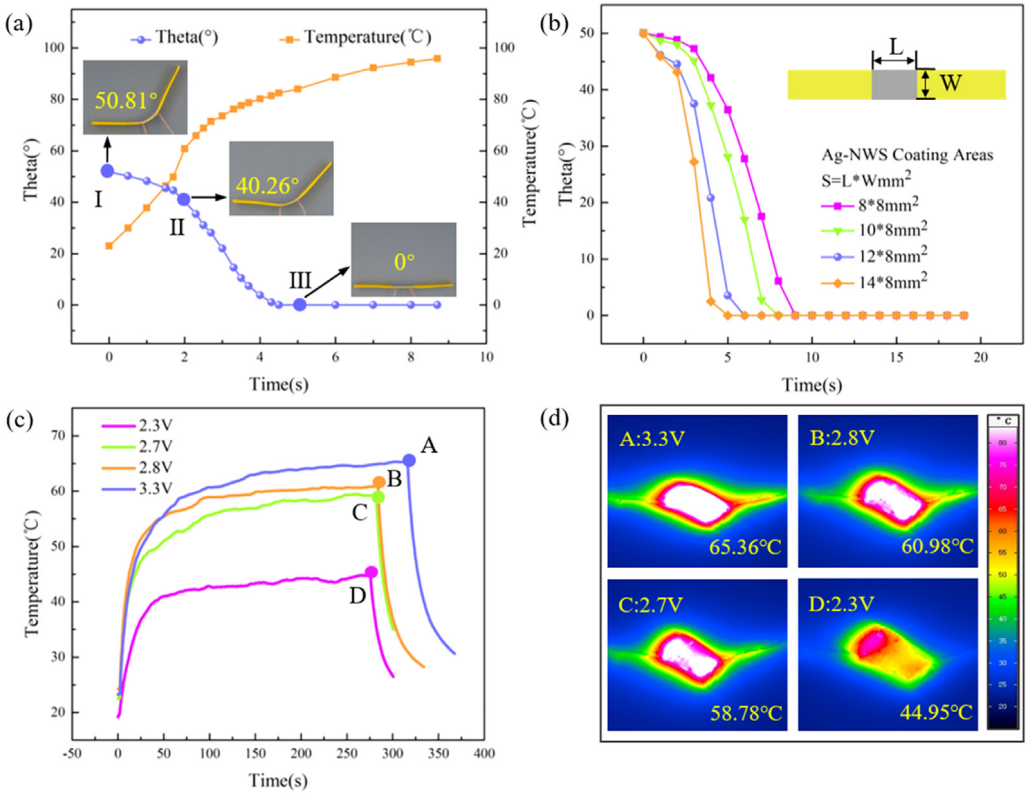

Fig. 2. The characterization of the applied electric power, temperature and deformation of the composite. (a) The relationship between the bending recovery angle (left) and temperature (right) variations versus the heating time of thin beam. (b) The bending recovery angle changes with heating time of the Ag-NWs with different areas. (c) The equilibrium temperature under different driving voltages. (d) The temperature distributions of the beam corresponding to four points A, B, C and D of Fig. 2(c).

where $t_2 = t - t_g$, α_{eff} is the effective thermal expansion coefficient, which can be calculated by Eq. (3) and the following equation [4]:

$$\varepsilon_p(t_2) = \left(\varepsilon_r - \varepsilon_g\right)\left(1 - e^{\frac{-t_2}{t_f}}\right) \tag{4}$$

where ε_r is the strain stored in pre-deformation.

The bending angle of the thin beam during the shape memory process is obtained:

$$\theta_2(x, t_2) = \theta_0 - \theta_g - 2\left(\varepsilon_r - \varepsilon_g\right)\left(1 - e^{\frac{-t_2}{t_f}}\right)\frac{x}{h} \tag{5}$$

where θ_g is the angle of recovery during the whole thermal expansion stage.

The previous work has explained how internal strain in PLA was generated during printing [5]. Similarly, we firstly evaluated the internal strain stored in PLA materials after pre-deformation. The strain of the strip during the deformation process was obtained by calculating the ratio of the contraction to the initial length. Then, the release of internal strain was recorded as shown in Fig. 3a when their temperature exceeds the T_g of PLA (60 °C). The moment $t = 0$ is corresponding to the heating started, during which time is the thermal expansion process till $t = T_g$. The theoretical strain and bending angle changing with time are plotted according to the above equations, which are compared with the experiment results as shown in Fig. 3. The experimental results agree well with the theoretical results, which both show the obvious transition points at the time of 2 s. At this point, the phase changing temperature, T_g of PLA is reached, which leads to the dramatically change of the deformation rate.

As we introduced in the method section, the major filler was the Ag-NWs. In order to be against the oxidation of Ag-NWs, a very thin layer of CSP was brushed on top. One can also choose other organic matter to protect Ag-NWs. In order to

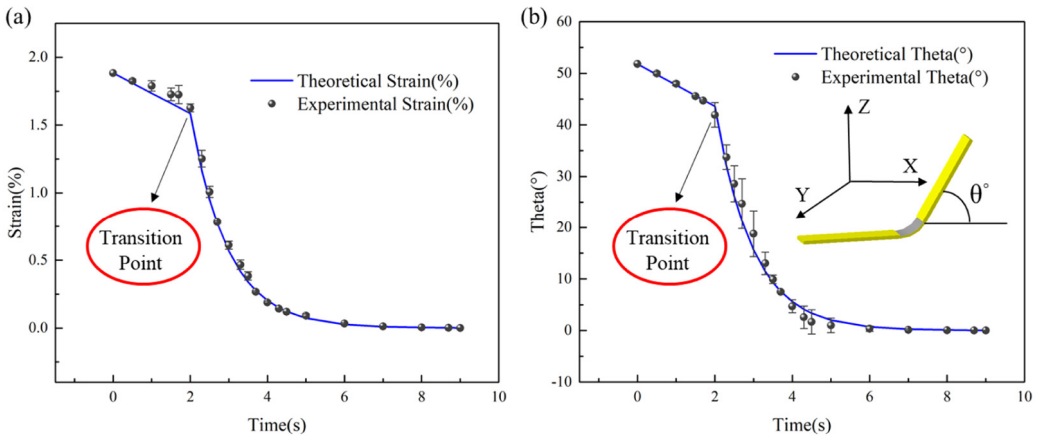

Fig. 3. Experimental and theoretical results of (a) strain and (b) bending angle changing with time of the thin beam.

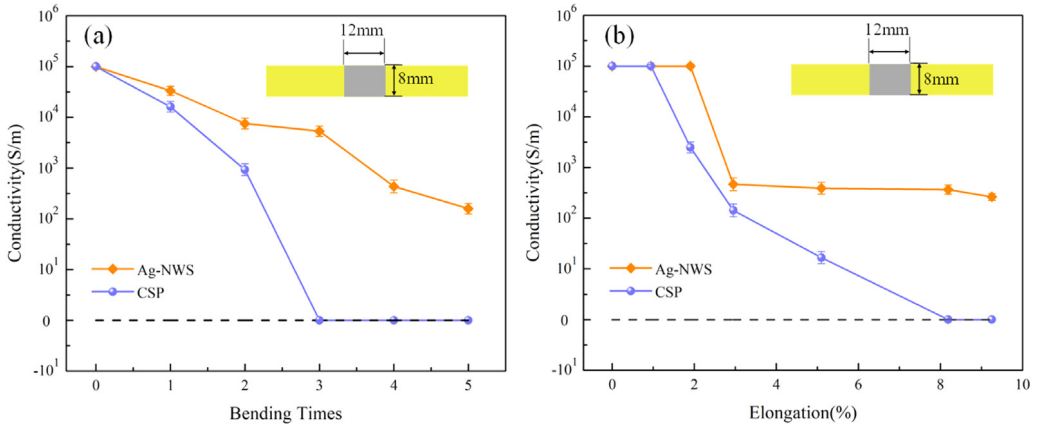

Fig. 4. Comparison of electrical conductivity after mechanical test. (a) Conductivity of the composite after thermodynamic bending test with the bending degree of 90 degrees. (b) Conductivity of the composite after tensile test.

compare the change of electrical conductivity of different fillers after several large deformations, the bending tests were taken on the thin beams with different fillers. The thin beam model with the dimension of $60\times8\times0.4$ mm^3, and with a groove of $12\times8\times0.1$ mm^3 in the middle which was coated with fillers. One model was only coated with CSP, the other was mainly coated with Ag-NWs and thin CSP layer on top, but the total quality of the Ag for each sample was the same. At the beginning, the conductivities of both fillers are 10^5 S/m. Then the beam was electro thermally pre-deformed to 90° followed by restoring to 0° both under an applied a voltage of 2.8 V, which is regarded as bending once. After the first bending test, the conductivity of the CSP decrease 83.87% as shown in Fig. 4(a), and no conductivity at all after the third time bending. In contrast, the conductivity of Ag-NWs filler decrease 66.67% after the third time bending and still keep a high conductivity (5319.149 S/m) after bending for three times, which illustrates the good bending resistance of the Ag-NWs filler.

Moreover, the tensile resistance of these two fillers are investigated. The thin beams were immersed in the water bath at 70 °C and stretched to different strain. As shown in Fig. 4(b), the conductivities of the Ag-NWs and CSP fillers dropped to 476.2 S/m and 200 S/m at 3% strain, respectively. The conductivity of CSP is 0 S/m when the strain is more than 8%, while that of Ag-NWs is nearly unchanged. Under stretching, the silver particles in CSP are separated apart and even disconnected to a great extent, which leads to the dramatic decrease of the electrical resistance of CSP. In contrast, Ag-NWs network could maintain excellent connection, thus the relative stable conductivity.

A biomimetic flower was designed as shown in Fig. 5(a). The flower consists of five petals, which are fixed on the support separately. Each petal could be controlled independently. After applied a 4 V voltage, each petal could be pre-deformed as desired. Similarly, the petal could also be open as designed by applying the required voltage. When heated to the temperature of T_g, the petals were expanded one by one in order, and finally the initial shape was restored (as shown in video 1). The petals could also expand together by applying the voltage at the same time (as shown in video 2).

Compared with the traditional pre-deformation methods such as water bath heating or hot stage heating, this method can make the structure get rid of the support of the solid platform to achieve a certain degree of freedom (line suspension heating), which make it adaptive to complex environments. In this way, the desired function can be realized by the SMP/Ag-NWs composite structure in different environments.

The gripper is an important application of SMP [34]. Therefore, an application of the SMP/Ag-NWs composite structure as a gripper in cold environment is demonstrated in Fig. 5(b). The heating without destroying the cold environment is hard to realize with the traditional methods, such as hot water bath and hot stage. Here, the gripper was mainly composed of three bending thin beams, which can be independently controlled. The beams were printed with a tiny curve of 150°. At the beginning, the gripper were pre-deformed by applying a voltage of 4.5 V till the beams becoming straight. Then, the beams were applied the same voltage to restore to the initial shape to grab the ball ($m = 2.7$ g)

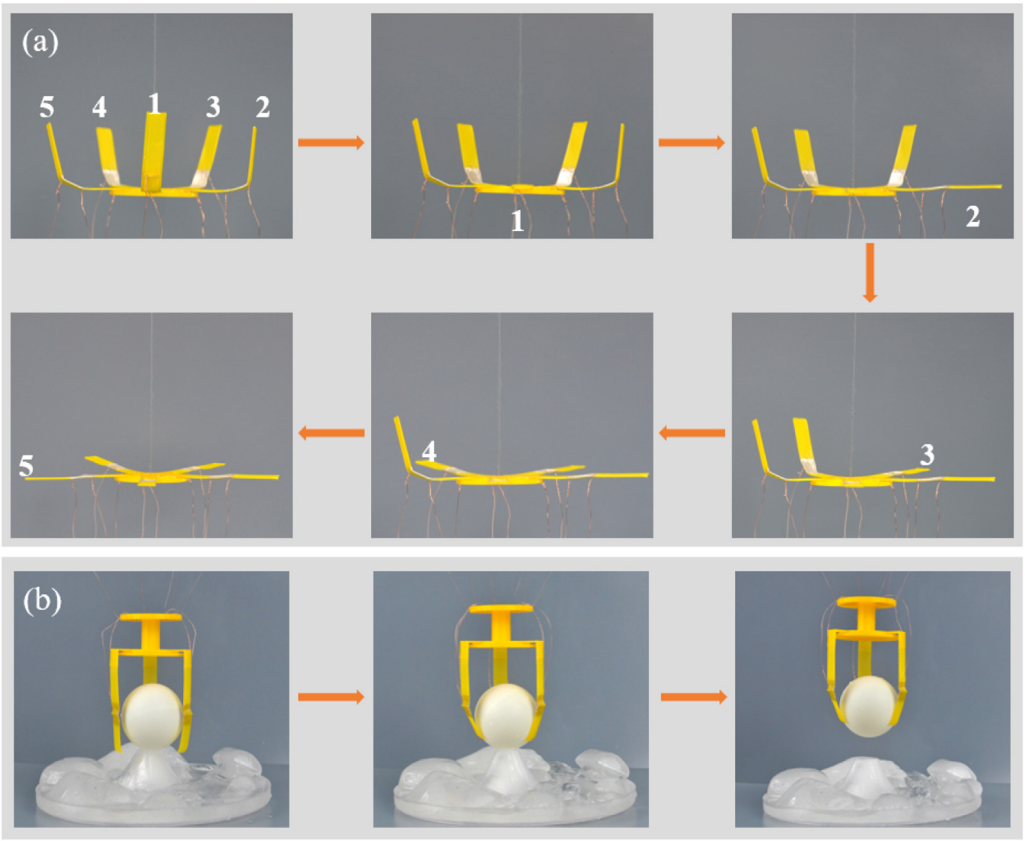

Fig. 5. The environment independent applications of the electrically controlled PLA/Ag-NWs composite structure with local deformation. (a) A biomimetic flower with five petals, and each petal could be independently expanded under the applied voltage. (b) A gripper grabbed a ball from the icy cold environment. Note that both applications cannot be realized by the traditional hot water bath or hot stage heating.

from icy environment (as shown in video 3). In this way, we do not need to put the whole structure in the thermal environment as the traditional method, which has great significance for the future application of shape memory composite materials at low temperature. The method in our work can be further combined with the hybrid printing [35,36], which could more precisely control the 3D printed structures to achieve the multifunction.

4. Conclusions

To summarize, the Ag-NWs and PLA was combined to develop a new 4D printing composite for electrically controlled local deformation. The composite had been shown to own two deformation processes upon applying a voltage, namely the thermal expansion and phase changing. The shape changing was fast as soon as the temperature achieving the phase changing temperature of the PLA. The minimum electric power was ca. 4.704 W to realize the phase change deformation of PLA/Ag-NWs structure. A biomimetic flower with five petals was presented, and each petal could be independently expanded under the applied voltage. In particular, a gripper functionalized in cold environment was shown. The method in this work could be used for different kind of SMP and the corresponding 4D printing composite and structures would be promising for applications in the fields of robots, temperature sensors, biomedicine, folded wings of deformable aircraft and so on.

Declaration of competing interest

The authors declare that they have no known competing financial interests or personal relationships that could have appeared to influence the work reported in this paper.

Acknowledgment

This work was supported by the National Natural Science Foundation of China (NSFC No. 11572051, 51501011, 11991031).

Appendix A. Supporting information

Supplementary material related to this article can be found online at https://doi.org/10.1016/j.eml.2020.100793.

Three videos have been provided as the Supplementary material.

References

[1] X. Kuang, D.J. Roach, J. Wu, et al., Advances in 4D printing: Materials and applications, Adv. Funct. Mater. 29 (2) (2019) 1805290.
[2] E. Pei, G.H. Loh, Technological considerations for 4D printing: an overview, Prog. Addit. Manuf. 3 (1–2) (2018) 95–107.
[3] Z. Ding, C. Yuan, X.R. Peng, et al., Direct 4D printing via active composite materials, Sci. Adv. 3 (2017) e1602890.
[4] Q. Zhang, D. Yan, K. Zhang, et al., Pattern transformation of heat-shrinkable polymer by three-dimensional (3D) printing technique, Sci. Rep. 5 (2015) 8936.
[5] Q. Zhang, K. Zhang, G. Hu, Smart three-dimensional lightweight structure triggered from a thin composite sheet via 3D printing technique, Sci. Rep. 6 (2016) 22431.
[6] S. Akbari, A.H. Sakhaei, K. Kowsari, et al., Enhanced multimaterial 4D printing with active hinges, Smart Mater. Struct. 27 (6) (2018) 065027.
[7] M. Zarek, M. Layani, I. Cooperstein, et al., 3D printing of shape memory polymers for flexible electronic devices, Adv. Mater. 28 (22) (2016) 4449–4454.
[8] C.M. Gonzalez-Henriquez, M.A. Sarabia-Vallejos, J. Rodriguez-Hernandez, Polymers for additive manufacturing and 4D-printing: Materials, methodologies, and biomedical applications, Prog. Polym. Sci. 94 (2019) 57–116.

[9] H. Yuk, S.T. Lin, C. Ma, et al., Hydraulic hydrogel actuators and robots optically and sonically camouflaged in water, Nature Commun. 8 (2017) 14230.
[10] Y. Kim, H. Yuk, R.K. Zhao, et al., Printing ferromagnetic domains for untethered fast-transforming soft materials, Nature 55 (2018) 274–279.
[11] B.Y. Lu, H. Yuk, S.T. Lin, et al., Pure PEDOT:PSS hydrogels, Nature Commun. 10 (2019) 1043.
[12] R. Temmer, A. Maziz, C. Plesse, et al., In search of better electroactive polymer actuator materials: PPy versus PEDOT versus PEDOT–PPy composites, Smart Mater. Struct. 22 (10) (2013) 104006.
[13] J.M. Jani, M. Leary, A. Subic, et al., A review of shape memory alloy research, applications and opportunities, Mater. Des. 56 (4) (2014) 1078–1113.
[14] M. Raja, S.H. Ryu, A.M. Shanmugharaj, Thermal, mechanical and electroactive shape memory properties of polyurethane (PU)/poly (lactic acid) (PLA)/CNT nanocomposites, Eur. Polym. J. 49 (11) (2013) 3492–3500.
[15] Y. Yang, Y. Chen, Y. Wei, et al., 3D printing of shape memory polymer for functional part fabrication, Int. J. Adv. Manuf. Technol. 84 (9–12) (2016) 2079–2095.
[16] S.T. Ly, J.Y. Kim, 4D printing–fused deposition modeling printing with thermal-responsive shape memory polymers, Int. J. Precis. Eng. Manuf.-Green Technol. 4 (3) (2017) 267–272.
[17] Q. Ge, A.H. Sakhaei, H. Lee, et al., Multimaterial 4D printing with tailorable shape memory polymers, Sci. Rep. 6 (2016) 31110.
[18] L. Sun, W.M. Huang, Z. Ding, et al., Stimulus-responsive shape memory materials: A review, Mater. Des. 33 (none) (2012) 577–640.
[19] C.L. Huang, M.J. He, M. Huo, et al., A facile method to produce PBS-PEG/CNTs nanocomposites with controllable electro-induced shape memory effect, Polym. Chem. 4 (14) (2013) 3987–3997.
[20] L. Yu, Q. Wang, J. Sun, et al., Multi-shape-memory effects in a wavelength-selective multicomposite, J. Mater. Chem. A 3 (26) (2015) 13953–13961.
[21] K. Yu, K.K. Westbrook, P.H. Kao, et al., Design considerations for shape memory polymer composites with magnetic particles, J. Compos. Mater. 47 (1) (2013) 51–63.
[22] A. Javed, K. Aslam, A. Manawwer, et al., Electroactive shape memory property of a Cu-decorated CNT dispersed PLA/ESO nanocomposite, Materials 8 (9) (2015) 6391–6400.
[23] L. Ma, J. Zhao, X. Wang, et al., Effects of carbon black nanoparticles on two-way reversible shape memory in crosslinked polyethylene, Polymer 56 (2015) 490–497.
[24] H. Lu, Y. Yao, W.M. Huang, et al., Significantly improving infrared light-induced shape recovery behavior of shape memory polymeric nanocomposite via a synergistic effect of carbon nanotube and boron nitride, Composites B 62 (2014) 256–261.
[25] J.T. Kim, B.K. Kim, E.Y. Kim, et al., Synthesis and shape memory performance of polyurethane/graphene nanocomposites, React. Funct. Polym. 74 (2014) 16–21.
[26] J. Guo, Z. Wang, L. Tong, et al., Shape memory and thermo-mechanical properties of shape memory polymer/carbon fiber composites, Composites A 76 (2015) 162–171.
[27] J.L. Rueda, C. Salas, Stretchable heater using ligand-exchanged silver nanowire nanocomposite for wearable articular thermotherapy, ACS Nano 9 (6) (2015) 6626–6633.
[28] T. Araki, J. Jiu, M. Nogi, et al., Low haze transparent electrodes and highly conducting airdried films with ultra-long silver nanowires synthesized by one-step polyol method, Nano Res. 7 (2) (2014) 236–245.
[29] W.M. Schuette, W.E. Buhro, Polyol synthesis of silver nanowires by heterogeneous nucleation; Mechanistic aspects influencing nanowire diameter and length, Chem. Mater. 26 (22) (2014) 6410–6417.
[30] X.Z. Xiang, W.Y. Gong, M.S. Kuang, et al., Progress in application and preparation of silver nanowires, Rare Met. 35 (4) (2016) 289–298.
[31] D. Doganay, S. Coskun, C. Kaynak, et al., Electrical, mechanical and thermal properties of aligned silver nanowire/polylactide nanocomposite films, Composites B 99 (2016) 288–296.
[32] F. Cock, A.A. Cuadri, M. García-Morales, et al., Thermal, rheological and microstructural characterisation of commercial biodegradable polyesters, Polym. Test. 32 (4) (2013) 716–723.
[33] H. Tobushi, T. Hashimoto, S. Hayashi, et al., Thermomechanical constitutive modeling in shape memory polymer of polyurethane series, J. Intell. Mater. Syst. Struct. 8 (8) (1997) 711–718.
[34] Q. Ze, X. Kuang, S. Wu, et al., Magnetic shape memory polymers with integrated multifunctional shape manipulation, Adv. Mater. 32 (2020) 1906657.
[35] X. Kuang, D.J. Roach, J. Wu, et al., Advances in 4D printing: Materials and applications, Adv. Funct. Mater. 29 (2) (2019) 1805290.
[36] E. Pei, G.H. Loh, Technological considerations for 4D printing: an overview, Prog. Addit. Manuf. 3 (1–2) (2018) 95–107.